A new particle-tracking approach to simulating transport in heterogeneous fractured porous media

Delphine Roubinet, Hui-Hai Liu, Jean-Raynald de Dreuzy

A new particle-tracking approach to simulating transport in heterogeneous fractured porous media

Delphine Roubinet,[1] Hui-Hai Liu,[2] and Jean-Raynald de Dreuzy[1]

Received 28 March 2010; revised 13 July 2010; accepted 9 August 2010; published 3 November 2010.

[1] Particle-tracking methods are often used to model contaminant transport in fractured porous media because they are straightforward to implement for fracture networks and are able to take into account the matrix effect without mesh generation. While classical methods assume infinite matrix or regularly spaced fractures, we have developed a stochastic method adapted to solute transport in complex fracture networks associated with irregular matrix blocks. Diffusion times in the matrix blocks are truncated by the finite size of the blocks. High ratios of matrix diffusion to fracture advection, small fracture apertures, and small blocks favor the transfer of particles to nearby fractures through matrix diffusion. Because diffusion occurs on both sides of the originating fracture before particles reach one of the neighboring fractures, transfer times to both neighboring fractures are strongly affected by the network configurations on both sides of the fracture. This new particle-tracking method is able to deal with complex fracture networks by considering heterogeneous configurations on both sides of the fracture. We finally show on simple Sierpinski lattice structures that neglecting the finite size of the matrix blocks may lead to orders of magnitude overestimations of the transfer times.

Citation: Roubinet, D., H.-H. Liu, and J.-R. de Dreuzy (2010), A new particle-tracking approach to simulating transport in heterogeneous fractured porous media, *Water Resour. Res.*, *46*, W11507, doi:10.1029/2010WR009371.

1. Introduction

[2] Exchanges between fracture and matrix have been recognized as a major issue for modeling solute transport in fractured media [*Carrera et al.*, 1998; *Neretnieks*, 1980]. Solutes are quickly advected in highly permeable fractures while they may be trapped by diffusion in the surrounding matrix blocks. Upscaled transport laws result from the successive speedups in fractures and slowdowns in matrix blocks. Beyond the rate of exchanges, the key controlling parameter is the broad-range distribution of block sizes coming from widely scattered fracture lengths and correlation scales [*Bonnet et al.*, 2001; *Bour and Davy*, 1999; *Davy et al.*, 2006; *Davy*, 2010; *Neuman*, 2005]. Most modeling frameworks relying on double porosity concepts [*Warren et al.*, 1963], however, are considering a limited scattering of block sizes and shapes. Some continuous approaches, as the multiple interacting continua approach [*Pruess and Narasimhan*, 1985], are able to deal with block shape and size variability by using a proximity function. However, this representation is applicable for fracture networks dense enough to be modeled by a continuum medium and requires large computational developments and resources due to the several levels of matrix block discretization. Other approaches based on a discrete representation of the fractures generally called discrete fracture network (DFN) can theoretically account for the more intricate and nested organization of the matrix blocks. Because of the geometrical complexity of the block shapes, DFN fracture matrix approaches implement mesh-free numerical methods like particle tracking where the presence of the matrix is integrated into a retardation time of the particles [*Cvetkovic et al.*, 2004; *Dershowitz and Miller*, 1995].

[3] The retardation time has been initially modeled by considering that all particles leaving a given fracture will return to this same fracture and will not transfer to other fractures. In this case, the retardation time is deduced from the classical solution by *Tang et al.* [1981] assuming a single fracture surrounded by an infinite matrix. Based on the solution of parallel and regularly spaced fractures [*Sudicky and Frind*, 1982], the method has been extended to account for nearby fractures [*Liu et al.*, 2000; *Shan and Pruess*, 2005]. Diffusion times become bounded by the presence of nearby fractures toward which particles can be transferred. This advanced method has still the major shortcoming of relying on highly regular fracture configurations precluding any block shape variability.

[4] We propose hereafter to further extend the particle-tracking method to account for general block shape configurations. The proposed particle-tracking method does not rely on an analytical solution of the diffusion equation but directly on the definition of a stochastic process with relevant boundary conditions. The method is applicable to heterogeneous fractured porous media without restriction on fracture geometry or network density. We present in section 2 the stochastic process valid both in 2D and 3D. Sections 3 and 4 show validation and illustration cases of the

[1] Géosciences Rennes, UMR CNRS 6118, Université de Rennes I, Rennes, France.
[2] Earth Sciences Division, Lawrence Berkeley National Laboratory, Berkeley, California, USA.

0043-1397/10/2010WR009371

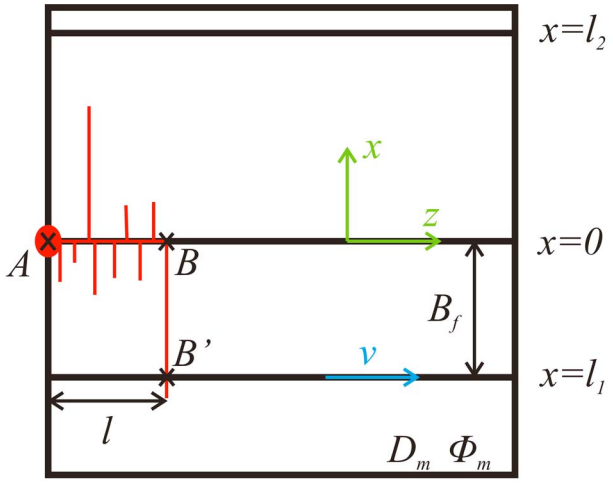

Figure 1. Notations for the particle-tracking method. Here x and z are the particle positions in the matrix and in the fracture, respectively, D_m and ϕ_m are the matrix diffusion and porosity, v is the fluid velocity in the fracture, B_f is the fracture spacing, and l is the distance traveled in the fracture. The initial fracture is at position $x = 0$ and its neighboring fractures are at positions $x = l_1 < 0$ and $x = l_2 > 0$. The red lines represent the particle displacement by 1D diffusion in the matrix and by advection in the fracture. The particle starts at position A and arrives at position B' (case of transfer), with B' the orthogonal projection of B onto the neighboring fracture. The advection time required for travel from A to B is the time step of the algorithm for which the diffusion time, corresponding to several entering the matrix, is studied.

method in 2D and sections 5 and 6 are devoted to discussion and conclusion.

2. Theory and Method

[5] The method has been developed for steady state flow conditions. Matrix diffusion is assumed to be 1D and perpendicular to fractures. We denote z and x the particle position in the fracture and in the matrix, respectively (Figure 1). For simplicity, we assume purely advective transport in fractures with homogeneous concentration across the width of the fracture. Similar assumptions have been used for developing analytical solutions for solute transport in fracture matrix systems [*Sudicky and Frind*, 1982; *Tang et al.*, 1981]. We show successively how particles diffuse into the matrix and come back to their originating fracture or are transferred to nearby fractures. We quantify the associated probabilities and transient times.

2.1. Diffusion Times for Single Fractures Embedded in an Infinite Matrix

[6] The case of a single fracture in an infinite surrounding matrix is valid when diffusion in the matrix occurs on distances smaller than the characteristic scale of the block. This condition is satisfied when transport is more controlled by the advection in the fracture than by the diffusion in the matrix. The cumulative distribution of the particle diffusion time in the infinite matrix for a given advection time t_a in the fracture is [*Liu et al.*, 2006; *Painter and Cvetkovic*, 2005]

$$P(t < T) = erfc\left(\frac{\phi_m\sqrt{D_m}}{2b\sqrt{T}}t_a\right) \quad (1)$$

with b the half aperture of the fracture, ϕ_m the surrounding matrix porosity and D_m the local matrix diffusion coefficient (D_m is the molecular diffusion coefficient multiplied by the tortuosity factor [*Bear*, 1979]). This formulation, based on the assumption of diffusion in a virtually infinite matrix, assumes that particles go back to the same fracture after their diffusion within the matrix.

[7] From equation (1), the diffusion time t_{diff} is modeled as a series of independent identically distributed random variables

$$t_{diff} = \left(\frac{\phi_m\sqrt{D_m}}{2\alpha b}t_a\right)^2 \quad (2)$$

with $\alpha = erfc^{-1}(U[0,1])$ and $U[0,1]$ a uniform random number in the interval [0,1]. Note that equation (2) is obtained by replacing $P(t < T)$ in equation (1) with $U[0,1]$.

[8] The matrix is assumed "infinite" only when the average diffusion distance perpendicular to the fracture $\overline{x_{diff}}$ is smaller than the fracture spacing B_f

$$\overline{x_{diff}} = \sqrt{2D_m\overline{t^*_{diff}}} = \frac{\phi_m D_m}{\sqrt{2}\alpha b}t_a < B_f \quad (3)$$

where $\overline{t^*_{diff}}$ is the average of t^*_{diff} with $t^*_{diff} = \frac{t_{diff}}{2}$ the time necessary to reach a penetration depth in the matrix equal to x_{diff}. By comparison, t_{diff} is the time needed to reach a distance x_{diff} plus the time needed to go back to the originating fracture. This statement is not strictly valid for a single particle but is satisfied for a large number of particles. By defining the Péclet number as $Pe = \frac{lv}{D_m}$, where l is the distance traveled in the fracture during the advection time t_a with the velocity v (Figure 1), the condition (3) of "infinite matrix" is valid only for large values of the Péclet number (dominance of advection in the fracture over diffusion in the matrix):

$$Pe > \frac{\phi_m l^2}{\sqrt{2}\alpha b B_f}. \quad (4)$$

For smaller values of the Péclet number, the assumption of infinite matrix breaks down and particles may transfer to the nearby fractures through the matrix.

2.2. Transfer Probabilities and Diffusion Times to Nearby Fracture(s)

[9] When condition (4) is not satisfied, the particle may be transferred to a nearby fracture. We determine the probability of transfer to the ith neighboring fracture $P^i_{transfer}$ and the probability of return to the originating fracture as well as the corresponding transfer times $t_{transfer}$. The probability of leaving the originating fracture $P_{transfer}$ is equal to the sum of the $P^i_{transfer}$.

[10] We consider a fracture at position $x = 0$ with two parallel neighboring fractures at positions $x = l_1 < 0$ and $x = l_2 > 0$, respectively (Figure 1). We denote $P^1_{transfer} = P(l_1, \overline{l_2},$

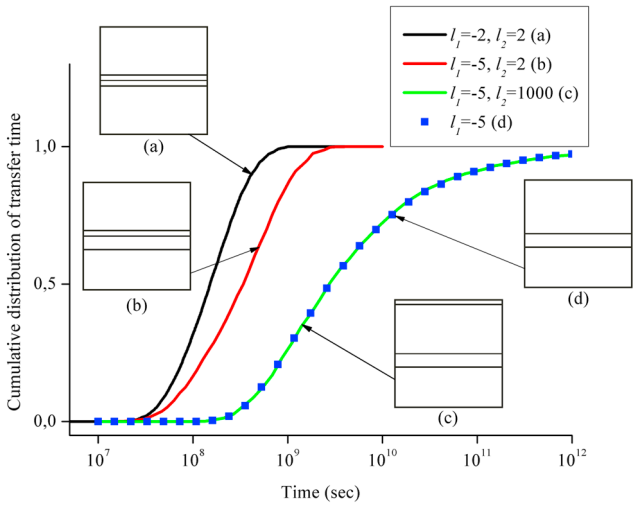

Figure 2. Cumulative distribution of the transfer time to nearby fractures. Particles transfer from position $x = 0$ to positions $x = l_1$ and $x = l_2$. Solid lines and dots represent results obtained with Feller and FPTD formulations, respectively. The local diffusion coefficient is equal to 10^{-8} m^2/s, and the fracture positions are expressed in meters.

$t_{transfer} \le t^*_{diff}$) the probability for a particle to transfer from position $x = 0$ to position $x = l_1 < 0$ without crossing the position $x = l_2 > 0$ before the time t^*_{diff} and $P^2_{transfer} = P(l_2, \overline{l_1}, t_{transfer} \le t^*_{diff})$ the probability for a particle to transfer to $x = l_2$ without crossing the position $x = l_1$ before the time t^*_{diff}. From *Feller* [1954], these probabilities are expressed in the Laplace space by the following expressions:

$$L\left(P^1_{transfer}\right) = \frac{\exp\left(l_1\sqrt{\lambda/D_m}\right)}{\lambda}\frac{1-\exp\left(-2l_2\sqrt{\lambda/D_m}\right)}{1-\exp\left(2(l_1-l_2)\sqrt{\lambda/D_m}\right)} \quad (5)$$

$$L(P^2_{transfer}) = \frac{\exp\left(l_2\sqrt{\lambda/D_m}\right)}{\lambda}\frac{1-\exp\left(-2l_1\sqrt{\lambda/D_m}\right)}{1-\exp\left(2(l_2-l_1)\sqrt{\lambda/D_m}\right)} \quad (6)$$

with $L()$ the Laplace transform defined by $L(f(t)) = \int_0^{+\infty} e^{-\lambda t} f(t)\, dt$. A sketch of the conceptual model is proposed in Figure 1. The particle crosses several times its originating fracture before reaching one of the two neighboring fractures. $P^1_{transfer}$ is larger than $P^2_{transfer}$ since $|l_1| < |l_2|$. Particle behavior is nonsymmetric along the initial fracture since more than 50% of the transferred particles reach the nearest fracture with small transfer times in comparison to the farthest fracture. The irregular fracture spacing also induces strong modifications in the mean position and shape of the transfer time distribution (Figure 2). Compared to the symmetric configuration (black curve), arrival in the asymmetric case (red curve) is delayed by half an order of magnitude. Because diffusion occurs on both sides of the originating fracture before the particle reaches one of the neighboring fractures as sketched in Figure 1, transfer to both neighboring fractures is largely delayed even if only one of the distances to the nearby fractures is increased. Increase of only one of the distances also affects the shape of the transfer time distribution by yielding significantly larger arrival times (green curve and blue dots of Figure 2).

[11] For parallel regularly spaced fractures, $|l_1| = |l_2|$, the probabilities $P^1_{transfer}$ and $P^2_{transfer}$ are equal, the particle behavior on each side is symmetric along the initial fracture and the solution is equal to the one of *Sudicky and Frind* [1982]. Furthermore, if the second fracture is extremely far from the initial position ($l_1 = l < 0$ and $l_2 = +\infty$), $P^2_{transfer}$ tends to 0 and $P^1_{transfer}$ tends to the following first passage time distribution (FPTD) [*Feller*, 1965]:

$$P^1_{transfer} = P\left(x = l_1, t_{transfer} \le t^*_{diff}\right) = 2P\left(Y_{*_{t_{diff}}} \ge l_1\right)$$
$$= 2\left(1 - P\left(Y_{*_{t_{diff}}} < l_1\right)\right) = 1 - erf\left(\frac{l_1}{2\sqrt{D_m t^*_{diff}}}\right). \quad (7)$$

This case is illustrated by the last configurations in Figure 2 for which the transfer time distribution is obtained by the Feller formulation (5) and (6) (green curve) and the FPTD formulation (7) (blue dots). The superposition of the curves shows that the upper matrix side is virtually "infinite" as particles do not transfer to the upper fracture before reaching the lower one.

2.3. Particle-Tracking Procedure

[12] We consider a segment AB of the initial fracture with a particle starting at position A (Figure 1). Assuming that the particle goes from A to B, a reference diffusion time t_{diff} is determined from equation (2) as if the fracture were embedded in an infinite matrix. Transfer to the ith neighboring fracture occurs with the probability $P^i_{transfer}$ and the required time $t_{transfer}$ is derived from equations (5) and (6). In this case, the particle travels from A to B' with B' the orthogonal projection of B onto the arrival fracture (Figure 1) and the travel time is $t_{AB'} = t_a + t_{transfer}$. $t_{transfer}$ is drawn from the transfer time distribution $P^i_{transfer}$ truncated by the reference diffusion time t^*_{diff}. In the absence of analytical formulation in the time domain, these computations require numerical Laplace inversions performed using Stehfest's method [*Stehfest*, 1970]. In the particular case of a single neighboring fracture, transfer to the nearby fracture occurs with the probability $P^1_{transfer}$ and the required time $t_{transfer}$ is derived from equation (7). Transfer does not occur with a probability $1 - P^1_{transfer}$. In this latter case, the infinite matrix assumption is valid and the particle travel time from A to B is simply $t_{AB} = t_a + t_{diff}$.

[13] To maintain the simulation accuracy in the particle-tracking method, the length of the segment AB should be restricted to statistically prevent the occurrence of more than one transfer to nearby fractures. To this end, we restrict the advection along the fracture by statistically limiting the transfer probability to $p_{\lim}$. Considering the half diffusion time t^*_{diff}, this condition is expressed by limiting t^*_{diff} to the mean transfer time $\langle t_{transfer} \rangle$ as

$$P\left(t^*_{diff} \ge \langle t_{transfer} \rangle\right) = 1 - P\left(t^*_{diff} \le \langle t_{transfer} \rangle\right) \le p_{\lim}. \quad (8)$$

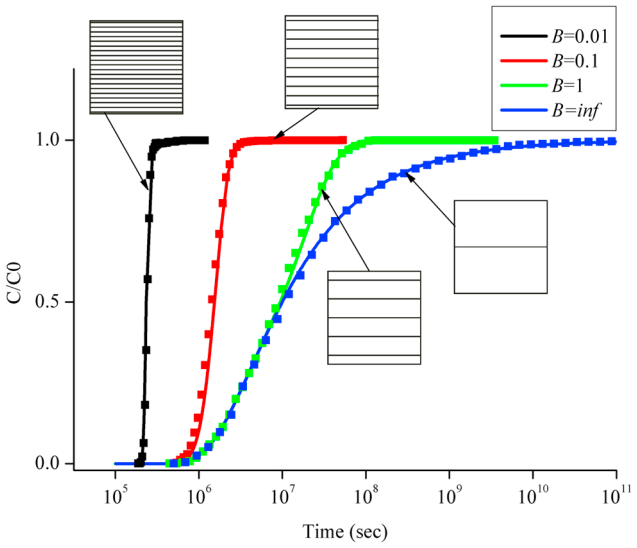

Figure 3. Breakthrough curves for a set of parallel fractures (black, red, and green curves) with different fracture spacings (B) and for a single fracture (blue curve). Solid lines and squares represent analytical solution and numerical results, respectively.

Using the stochastic expression of the analytical solution for a single fracture embedded in an infinite matrix (equation (1)), we obtain the following condition on advection time to ensure a transfer probability lower than $p_{\lim}$

$$t_a \leq \frac{2b\sqrt{\langle t_{transfer}\rangle}}{\phi_m\sqrt{D_m}} erfc^{-1}(1-p_{\lim}). \quad (9)$$

with the mean transfer time $\langle t_{transfer}\rangle$ obtained by using the backward Fokker-Planck equation and equal to the mean exit time of particles injected between two absorbing barriers [*Gardiner*, 2009]

$$\langle t_{transfer}\rangle = \frac{|l_1||l_2|}{2D_m}. \quad (10)$$

This particle-tracking method has been implemented in a software called PATH2 for Particle Tracking model for Highly Heterogeneous fractured porous media.

3. Validation

[14] The proposed model is validated for a single fracture embedded in an infinite matrix and a set of parallel fractures by comparing simulation results with analytical solutions [*Pan and Bodvarsson*, 2002; *Sudicky and Frind*, 1982; *Tang et al.*, 1981]. Figure 3 shows comparisons between analytical and numerical results for several different fracture spacings (black, red and green curves) and for a single fracture system (blue curve). In these examples, the distance between inlet and outlet points is 100 m, fluid velocity is 10^{-3} m/s, fracture aperture is 10^{-3} m, matrix diffusion coefficient is 10^{-8} m^2/s, and matrix porosity is 0.15. The upper boundary of the transfer probabilities $p_{\lim}$ (equation (9)) has been set to 0.1 by verifying that the results do not vary for lower values. The simulation results are very close to the analytical solutions, indicating that the proposed particle-tracking approach can accurately deal with solute transport involving solute particle transfer to neighboring fractures for regular configurations.

4. Illustration on Sierpinski Lattices

[15] As an example of application, the software PATH2 is used to simulate solute transport in complex fracture networks with fractal properties and correlation between fracture length and position [*Bonnet et al.*, 2001; *Davy et al.*, 2006; *Doughty and Karasaki*, 2002; *Liu et al.*, 2004]. We use Sierpinski lattices as a model of hierarchical organization [*Doughty and Karasaki*, 2002]. We apply impervious boundary conditions and head gradient on the horizontal and vertical sides of the domain, respectively, inducing a mean fluid velocity of 10^{-3} m/s from the left side to the right side. Particles are tracked on these structures with a matrix porosity of 0.15, a local diffusion coefficient of 10^{-8} m^2/s and the relationship $2b = 10^{-5}l_f$ between fracture aperture $2b$ and fracture length l_f. The domain size L is 27 m. We perform three different Monte Carlo simulations with the length of the smallest fracture l_{min} equal to 9 m, 3 m and 1 m. Illustrations of single realizations are shown in the insets of Figure 4. The curves of the Figure 4 represent the cumulative distribution of the time required to reach the right side of the domain for particles injected on the left side. For comparison purposes, transport is first simulated by assuming infinite surrounding matrix (Figure 4, dashed lines), and second by using the software PATH2 allowing particle transfer to nearby fractures through the matrix (Figure 4, solid lines). Under the assumption of infinite surrounding matrix (Figure 4, dashed lines), the decrease in $l_{\min}$ induces breakthrough curves with larger arrival times but similar shape. It is mostly due to the enhancement of matrix diffusion compared to fracture advection for the smaller aperture b of the

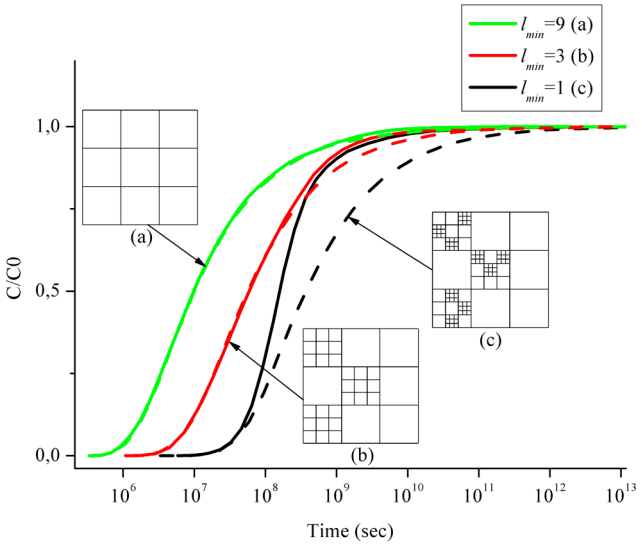

Figure 4. Breakthrough curves for hierarchical fracture networks with different fracture resolutions. The length of the smallest fracture ranges from 1 m to 9 m (from the green curves to the black curves) with a domain size of 27 m. Dashed lines show results assuming infinite matrix, whereas solid lines show results by accounting for the effect of the neighboring fractures.

smaller fractures (equation (1)). Allowing particle transfer (Figure 4, solid lines) significantly alters the shape of the breakthrough curve for the case l_{min} = 1 m only. It is only for the smallest explored distance between fractures corresponding to l_{min} ($B_f = l_{min}$) that particles can be transferred to neighboring fractures as the assumption of infinite matrix (equation (4)) becomes invalid for the smallest matrix blocks. Large matrix diffusion times are truncated by transfer to closer nearby fractures and the breakthrough curve becomes steeper (Figure 4, black solid line). Assuming an infinite matrix in this case leads to 1–2 orders of magnitude overestimation of the mean and standard deviation of arrival times. As previously stated in section 2, diffusion on both sides of the fractures is impacted by the presence of smaller matrix blocks through the increased probability of faster particle transfer to the nearest fracture.

5. Discussion

[16] The present particle-tracking method has been developed under the assumptions of steady state and uniform flow, pure advection in the fracture and 1D diffusion in the homogeneous matrix. Possible approximations of the method come from the fracture network discretization. From the DFN representation, the 2D fracture network is separated into segments delimited by fracture intersections and extremities. These segments, themselves, are divided in sections such as at most one transfer may occur for a particle traveling along a section. The condition on the section length, deduced from the equation (9), is not restrictive as the required section length will not be critically small for realistic fractured media.

[17] The method could also be adapted to less regular networks with nonparallel fractures. Over a given advective step within a fracture, we define on each side the characteristic transfer distance as the mean distance to the closest neighboring fracture. The method precision can be improved by restricting the advective step within the originating fracture.

[18] The presented model could be improved by a full representation of physical processes occurring in the fracture. Longitudinal dispersion effect could be integrated within the distribution of the diffusion times (equation (1)) by using the analytical solution developed for this case by *Tang et al.* [1981]. However, it seems more difficult to integrate transversal dispersion and/or Poiseuille profile within the fracture as it requires the development of an analytical solution to deduce the associated diffusion time distributions.

[19] After all, the most interesting challenge is the extension to 3D fractured porous media for field applications. As particle path is a succession of 1D displacement (even for 2D fractures represented by planes), the diffusion time distributions described in the theoretical part, and thus the conceptual model, are fully applicable to 3D media.

6. Conclusion

[20] To account for the effects of small-scale fractures and small matrix block sizes, it is critical to consider the impact of nearby fractures on solute transport. These small-scale fractures may not significantly contribute to global-scale water flow but may have significant effects on solute transport through matrix diffusion [*Liu et al.*, 2006]. To the best of our knowledge, the current study may represent the first effort in developing a particle-tracking algorithm that can handle effects of complex and widely scattered finite matrix blocks on solute transport in fractured porous media. With this simulation method, we intend to explore the effect of matrix diffusion on solute transport processes in complex fracture structures in order to better understand the origin of the scale dependence of the effective matrix diffusion coefficient [*Liu et al.*, 2004]. This method can be also used to improve site characterization by determining the impacts of fracture network structures on transport data.

[21] **Acknowledgments.** This project has been funded by the French National Research Agency ANR through the MICAS project (ANR-07-CIS7-004). The Brittany council is acknowledged for its financial contribution through a mobility grant.

References

Bear, J. (1979), *Hydraulics of Groundwater*, McGraw-Hill, London.

Bonnet, E., O. Bour, N. E. Odling, P. Davy, I. Main, P. Cowie, and B. Berkowitz (2001), Scaling of fracture systems in geological media, *Rev. Geophys.*, *39*(3), 347–383, doi:10.1029/1999RG000074.

Bour, O., and P. Davy (1999), Clustering and size distributions of fault patterns: Theory and measurements, *Geophys. Res. Lett.*, *26*(13), 2001–2004, doi:10.1029/1999GL900419.

Carrera, J., et al. (1998), On matrix diffusion: Formulations, solution methods and qualitative effects, *Hydrogeol. J.*, *6*(1), 178–190, doi:10.1007/s100400050143.

Cvetkovic, V., S. Painter, N. Outters, and J. O. Selroos (2004), Stochastic simulation of radionuclide migration in discretely fractured rock near the Äspö Hard Rock Laboratory, *Water Resour. Res.*, *40*, W02404, doi:10.1029/2003WR002655.

Davy, P. (2010), A likely universal model of fracture scaling and its consequence for crustal hydromechanics, *J. Geophys. Res.*, *115*, B10411, doi:10.1029/2009JB007043.

Davy, P., et al. (2006), Flow in multiscale fractal fracture networks, *Geol. Soc. Spec. Publ.*, *261*(1), 31–45, doi:10.1144/gsl.sp.2006.261.01.03.

Dershowitz, W., and I. Miller (1995), Dual-porosity fracture flow and transport, *Geophys. Res. Lett.*, *22*(11), 1441–1444, doi:10.1029/95GL01099.

Doughty, C., and K. Karasaki (2002), Flow and transport in hierarchically fractured rock, *J. Hydrol.*, *263*(1–4), 1–22, doi:10.1016/S0022-1694(02)00032-X.

Feller, W. (1954), Diffusion processes in one dimension, *Trans. Am. Math. Soc.*, *77*(1), 1–31.

Feller, W. (1965), *An Introduction to Probability Theory and Its Applications*, John Wiley, New York.

Gardiner, C. (2009), *Stochastic Methods*, Springer, Berlin.

Liu, H. H., G. S. Bodvarsson, and L. Pan (2000), Determination of particle transfer in random walk particle methods for fractured porous media, *Water Resour. Res.*, *36*(3), 707–713, doi:10.1029/1999WR900323.

Liu, H. H., et al. (2004), Scale dependency of the effective matrix diffusion coefficient, *Vadose Zone J.*, *3*(1), 312–315.

Liu, H. H., et al. (2006), An interpretation of potential scale dependence of the effective matrix diffusion coefficient, *J. Contam. Hydrol.*, *90*(1–2), 41–57, doi:10.1016/j.jconhyd.2006.09.006.

Neretnieks, I. (1980), Diffusion in the rock matrix: An important factor in radionuclide retardation, *J. Geophys. Res.*, *85*(B8), 4379–4397, doi:10.1029/JB085iB08p04379.

Neuman, S. P. (2005), Trends, prospects and challenges in quantifying flow and transport through fractured rocks, *Hydrogeol. J.*, *13*(1), 124–147, doi:10.1007/s10040-004-0397-2.

Painter, S., and V. Cvetkovic (2005), Upscaling discrete fracture network simulations: An alternative to continuum transport models, *Water Resour. Res.*, *41*, W02002, doi:10.1029/2004WR003682.

Pan, L. H., and G. S. Bodvarsson (2002), Modeling transport in fractured porous media with the random-walk particle method: The transient activity range and the particle transfer probability, *Water Resour. Res.*, *38*(6), 1080, doi:10.1029/2001WR000901.

Pruess, K., and T. N. Narasimhan (1985), A practical method for modeling fluid and heat-flow in fractured porous media, *SPEJ Soc. Pet. Eng. J.*, *25*(1), 14–26, doi:10.2118/10509-PA.

Shan, C., and K. Pruess (2005), An analytical solution for slug tracer tests in fractured reservoirs, *Water Resour. Res.*, *41*, W08502, doi:10.1029/2005WR004081.

Stehfest, H. (1970), Numerical inversion of Laplace transforms, *Commun. ACM*, *13*(1), 47, doi:10.1145/361953.361969. (Correction, Commun. ACM, *13*(10), 624, doi:10.1145/355598.362787, 1970.)

Sudicky, E. A., and E. O. Frind (1982), Contaminant transport in fractured porous media: Analytical solutions for a system of parallel fractures, *Water Resour. Res.*, *18*(6), 1634–1642, doi:10.1029/WR018i006p01634.

Tang, D. H., E. Frind, and E. Sudicky (1981), Contaminant transport in fractured porous media: Analytical solution for a single fracture, *Water Resour. Res.*, *17*(3), 555–564, doi:10.1029/WR017i003p00555.

Warren, J. E., et al. (1963), The behavior of naturally fractured reservoirs, *SPEJ Soc. Pet. Eng. J.*, *3*(3), 245–255.

J.-R. de Dreuzy and D. Roubinet, Géosciences Rennes, UMR CNRS 6118, Université de Rennes I, F-35042 Rennes, France. (delphine.roubinet@univ-rennes1.fr)

H.-H. Liu, Earth Sciences Division, Lawrence Berkeley National Laboratory, Berkeley, CA 94720, USA.